A Model-based Approach to Detect an Under-Lubricated Condition in a Ball Bearing

Ranjith-Kumar Sreenilayam-Raveendran[1], Michael H.Azarian[2], and Michael Pecht[3]

Center for Advanced Life Cycle Engineering (CALCE), University of Maryland, College Park, Maryland, USA

[1]*ranjith@calce.umd.edu*
[2]*mazarian@calce.umd.edu*
[3]*pecht@calce.umd.edu*

ABSTRACT

Bearings with an insufficient amount of lubricant can lead to early field failures, especially in applications which fail due to lubricant degradation, such as cooling fans used for thermal management of electronics. A reduced amount of lubricant can accelerate the wear process in the bearing, since there is not enough lubricant film thickness to support the operating load on the bearing. Qualification of bearings in cooling fans is carried out by time-truncated tests, where cooling fans have to operate without failure for a pre-determined period of time. Under-lubricated bearings can survive without failure in these tests leading to the usage of these bearings in the field resulting in field returns and warranty claims.

A non-linear dynamic model of a ball bearing is developed to simulate the transfer of load from the inner race to the outer race of the bearing as well as the acceleration signal as a function of time. An under-lubricated bearing condition is simulated in this model by changing the load transmitted to the outer race due to the reduced amount of lubricant. The simulated acceleration signal of the under-lubricated bearing condition is compared with that from the normal bearing to develop a fault-characteristic feature. The changes observed in the fault-characteristic feature from the simulation is validated by comparing with that obtained from experiments conducted on bearings with varying amounts of grease, ranging from none to the nominal amount specified by the manufacturer. The vibration level of these bearings was monitored at various operating speeds during the experiment. The changes observed in the fault-characteristic feature from the experiment due to a reduction of the lubricant in the bearing were similar to that observed in the simulations. This study resulted in the development of an experimental methodology and a fault-characteristic feature which can be used as a method for rapid acceptance testing of bearings. The dynamic model developed in this study can be used to determine the fault-characteristic feature for any bearing design.

1. INTRODUCTION

Bearings are used in machinery where the components in relative motion have to be supported on a stationary structure. For example, ball bearings are used to support a rotating shaft on a fixed structure. Bearing failures are the foremost cause for breakdown in rotating machinery: 40-50% of all industrial motor failures have been reported to be caused by bearings (Nandi, Toliyat, & Li, 2005), 43% of all cooling fan failures in electronic devices have been attributed to bearing failures (Kim, Vallarino, & Claassen, 1996), and longer down time during maintenance in wind turbines has been attributed to bearing failures (Ribrant & Bertling, 2007). Bearing fault diagnostics has been carried out to detect faults on the bearing components: the inner race, outer race, cage and the rolling elements. This is carried out by analyzing vibration signals obtained from a faulty bearing and comparison of the results with a bearing having no faults (Tandon & Choudhury, 1999). An insufficient lubrication condition in a bearing is also a fault condition which has not been studied extensively. Lubricants are used in the bearing to reduce the friction between bearing surfaces in relative motion. An improper lubrication condition in the bearing can be an over-lubricated condition, an under-lubricated condition or one with no lubricant in the bearing. The first case can increase the power required to maintain the motion of the rotating surfaces, since the excess lubricant increases the viscous drag forces in the bearing. The last two cases can accelerate the degradation process in the bearing since the lubricant film thickness is not sufficient to support the load acting on the bearing elements.

The relevant literature which pertains to bearing fault detection of an improper lubrication condition consists of the following two studies. Detection of bearings without any

lubricant has been accomplished using envelope analysis of their vibration signals (Boškoski, Petrovčič, Musizza, & Juričić, 2010). The frequency band selection for the envelope analysis was carried out based on spectral coherence and spectral kurtosis analysis. The amplitudes at the fundamental train frequency (FTF) and the ball spin frequency (BSF) were higher for the bearing without any lubricant compared to that with lubricant. Detection of an over-lubricated condition in the bearing has also been carried out in the literature (Morinigo-Sotelo, Duque-Perez, & Perez-Alonso, 2010). Tests were conducted on bearings with excess lubrication which were allowed to operate for 30 days, during which the excess lubricant was expelled from the bearing. The frequency spectrum of the stator electrical current of the motor driving the bearing was analyzed to detect the excess lubrication condition. Differences were observed in the amplitudes of the FTF and BSF in the electrical current spectrum between the excess lubricated and normal lubricated case of the bearing. Neither of these studies addressed the issue of detecting a bearing condition containing lubricant between the nominal amount and none at all. A reduction in the lubricant from the nominal amount can reduce the life of the bearing, resulting in earlier failures than that specified by the manufacturer. Qualification tests carried out on bearings can fail to detect this fault condition, especially if the test is a time-truncated test, where the bearing has to operate without failure for a specified period of time. An example of such a qualification test is the IPC-9591 standard used to qualify bearings used in cooling fans for electronics applications. Hence, the detection of an improper lubrication condition is of value in acceptance testing of bearings, and these tests would have to be carried out in a limited time in such a scenario. A model-based approach is adopted in this study for detection of an improper lubrication condition in a bearing. A dynamic model of the ball bearing components is created to simulate the rotational motion between the different components of a ball bearing. A fault condition is simulated using this model and the acceleration signal is compared with that of the normal lubrication condition. The simulation results are compared with results obtained from experiments using inadequately lubricated bearings.

2. BEARING MODEL

A dynamic model of the components of a ball bearing is developed assuming that the outer race is fixed. The transmission of forces between the individual components is modeled using a spring and damper system. In order to model the forces and deformation in the rolling contact between the components, Hertzian contact theory is used. The contact force for a point contact is given by the following relation:

$$f_b = k_b \delta^{1.5} \tag{1}$$

where k_b is the nonlinear bearing stiffness corresponding to the bearing deformation δ. The nonlinear bearing stiffness is a function of the bearing material and the bearing geometry. For point contact between two bodies made of the same material, the relation between contact deformation and contact force is given by the following relation:

$$\delta = 1.5\left(\frac{2K}{\pi\mu}\right)\sqrt[3]{\frac{1}{E}\left(1-\nu^2\right)\left(\frac{\sum\rho}{3}\right)}\, f_b^{\,2} \tag{2}$$

In this relation, bearing material properties are the Young's modulus (E) and the Poisson's ratio (ν). The Hertzian coefficients $\Sigma\rho$ and $2K/\pi\mu$ can be obtained from standard bearing tables based on the bearing contact geometry (Eschmann, Hasbargen, Weigand, & Brändlein, 1985). These coefficients are a function of the radius of curvature of the inner race, outer race and ball surfaces which are in contact. The contact deformation (δ) is obtained based on the displacement of the bearing in the x- and y-directions.

A force balance is carried out on the components of the bearing assuming a two degree-of-freedom system as shown in Figure 1.

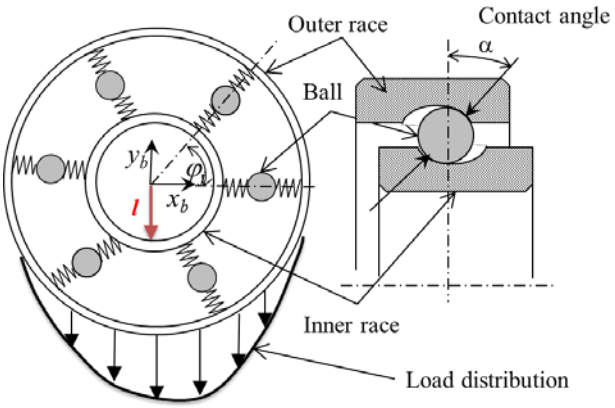

Figure 1. Schematic of two degree-of-freedom model of bearing system.

The governing equations of motion for this two degree-of-freedom system are shown in (3)-(6). The subscripts b_1 and b_2 in these equations correspond to the bearing located on a shaft s as shown in Figure 2. The bearings are located in a bushing and are held in position by means of a spring and washer. The shaft supported by the bearings is driven by a brushless DC motor which can rotate at a maximum speed of 4800 rpm.

$$m_{b1}\ddot{x}_{b1} + k_s\left(x_{b1} - x_{b2}\right) + q_s\left(\dot{x}_{b1} - \dot{x}_{b2}\right) + f_{b1x} = 0 \tag{3}$$

$$m_{b2}\ddot{x}_{b2} + k_s\left(x_{b2} - x_{b1}\right) + q_s\left(\dot{x}_{b2} - \dot{x}_{b1}\right) + f_{b2x} = 0 \tag{4}$$

$$m_{b1}\ddot{y}_{b1} + k_s\left(y_{b1} - y_{b2}\right) + q_s\left(\dot{y}_{b1} - \dot{y}_{b2}\right) + f_{b1y} = l \tag{5}$$

$$m_{b2}\ddot{y}_{b2} + k_s\left(y_{b2} - y_{b1}\right) + q_s\left(\dot{y}_{b2} - \dot{y}_{b1}\right) + f_{b2y} = l \quad (6)$$

The mass of the bearing is represented by *m*, transverse stiffness and damping of the shaft due to the axial load supported by the bearing is given by *k* and *q*, and load acting on each bearing is represented by *l*.

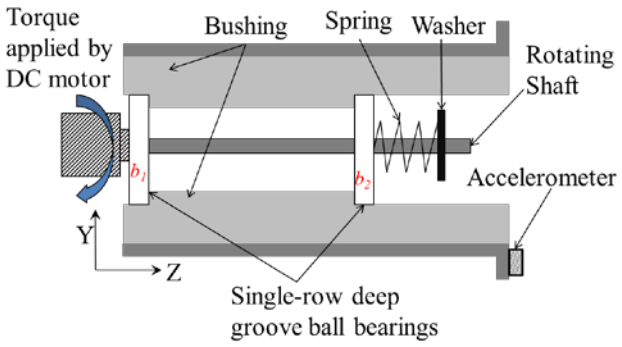

Figure 2. Schematic of bearing assembled on a shaft.

Solving the governing equations (3)-(6) as a function of time, the displacement of the bearing is calculated, from which the contact deformation δ is obtained. The contact deformation is calculated for each rolling element as shown in Figure 3 when the rolling element enters the load distribution zone shown in Figure 1. The relationship between contact deformation and bearing displacement is given by the following relation (Sawalhi & Randall, 2008):

$$\delta = \delta_x + \delta_y = x_b \cos\varphi + y_b \sin\varphi \quad (7)$$

The angular position of the j^{th} ball after a time increment *dt* is calculated from the cage rotational frequency using (8).

$$\varphi_j = \frac{2\pi\left(j-1\right)}{n_b} + \left(1 - \frac{D_b}{D_p}\cos\alpha\right)\frac{\omega_s}{2}dt \quad (8)$$

where n_b is the number of balls, D_b is the ball diameter, D_p is the pitch circle diameter of the balls, α is the contact angle and ω_s is the shaft rotational frequency.

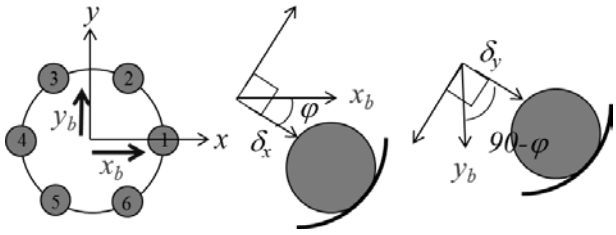

Figure 3. Relation between contact deformation (δ) and bearing displacement *x* and *y*.

In order to include the damping in the ball contact due to the presence of the lubricant, equation (1) is modified to include a viscoelastic damping contribution in addition to the elastic Hertzian component as shown below (Machado, Moreira, Flores, & Lankarani, 2012):

$$f_b = k_b\delta^n + \chi\delta^n\dot{\delta} \quad (9)$$

where χ is the contact damping factor, $\dot{\delta}$ is the rate of change of contact deformation and n = 1.5 in the case of a ball bearing.

3. MODEL SIMULATION

The system of equations explained in the previous section is used to develop a model in Matlab/Simulink®. This model is solved to obtain the time domain acceleration signal using the ode4 solver which is based on the Runge-Kutta method. The bearing parameters which are used in this model for simulation are shown in Table 1. The operating load acting on each bearing is 0.69 N.

Table 1. Bearing parameters used for simulation

Bearing parameters	Value
Number of rolling elements (n_b)	6
Diameter of rolling elements (d_b)	1.588 mm
Pitch diameter of bearing (d_p)	5.5 mm
Contact angle (α)	10.4°
Mass of bearing (m_b)	0.76 g
Young's modulus (E)	210 GPa
Poisson's ratio (ν)	0.3

An under-lubricated condition of the bearing results in the bearing elements operating in a boundary layer lubrication regime. This is due to a reduction in the lubricant film thickness supporting the load acting on the bearing. This results in the contact of asperities during relative movement of the surfaces, which causes the Hertzian pressure distribution to rise to 1.5 times that observed in an ideal Hertzian contact (Stachowiak & Batchelor, 2013). The under-lubricated bearing operation is simulated in the model by increasing the bearing stiffness and at the same time decreasing the damping in the contact due to the reduced lubricant film thickness. The values for the bearing stiffness and damping were estimated by calibrating the model based on the vibration signals measured from the experiment, which is discussed in the next section.

4. EXPERIMENTAL SECTION

The bearings used in this study were mounted in a fixture as shown in Figure 2 and were held in place by a spring-washer locking system. Vibration signals were measured while the bearings were operated at different speeds using a DC motor. The motor had a maximum speed of 4800 rpm. The speed of the cooling fan could be reduced down to 2160 rpm using a controller governed by a pulse width modulation (PWM) signal.

Bearings which contained the nominal amount of grease as specified by the manufacturer are referred to as 100% bearings in this study. The same experimental set up was used to test specially manufactured bearings which contained a reduced amount of grease. Bearings containing half of the nominal amount of grease are referred to as 50% bearings, and bearings containing a quarter of the nominal amount of grease are referred to as 25% bearings. Analysis of the vibration signals was carried out to develop a procedure to distinguish the bearings containing the nominal amount of grease from the others. Figure 4 shows root mean square (rms) acceleration of the bearings for different operating speeds. The highest vibration level for the 100% bearing was observed at 3815 rpm. For the 50% and 25% bearing, the highest vibration level was shifted to 3960 rpm. Another trend which can be observed is that the vibration level of the 50% bearing is higher than that of the 100% bearing at 3960 rpm, whereas the vibration level of the 25% bearing is similar to that of the 100% bearing.

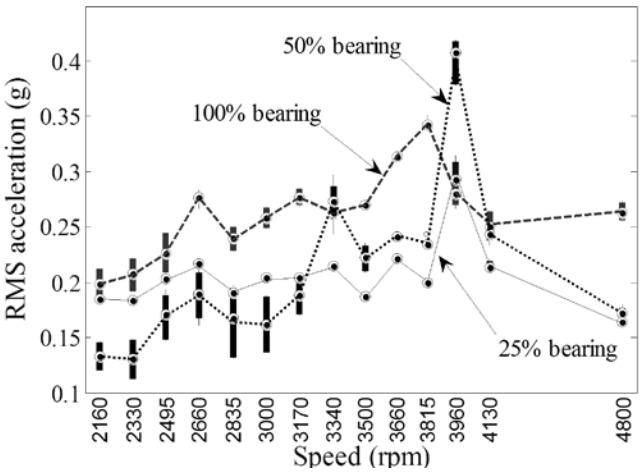

Figure 4. Box plot of rms acceleration at different bearing rotational speeds. The edges of the box at each data point are the 25th and 75th percentiles of the measurements and the whiskers correspond to +/-2.7σ assuming the data is normally distributed.

A feature for fault detection due to a reduction in the lubricant level of the bearing was developed based on the shift in the vibration level from one operating speed to another operating speed. The 100% bearing is used as a reference to develop this feature. The speed at which the maximum vibration level is observed is selected as the reference speed (3815 rpm from Figure 4). The speed at which the maximum vibration level is observed for the under-lubricated bearing is then selected to develop the fault feature, which is the ratio of the vibration level observed at 3815 rpm to the vibration level at the speed at which maximum vibration is observed for the underlubricated bearing. Figure 5 shows the fault feature used for classification. When this ratio is greater than 1 the bearing can be classified as a 100% bearing. A bearing with a ratio less than 1 can be classified as a faulty bearing. This fault feature can be used for classification of bearings with reduced amount of lubricant from that of the nominal bearings. This fault feature is quick to measure and can be readily implemented in an acceptance test scenario for bearings.

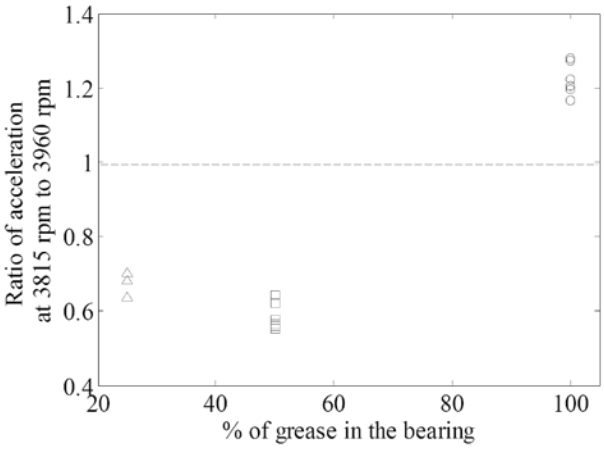

Figure 5. Fault feature for classification of amount of grease in a bearing

5. MODEL CALIBRATION

In order to explain the variations in vibration level with a reduction in the lubricant in the bearing, the bearing stiffness and damping values were calibrated in the model to identify the values which will generate the same vibration level as that observed in the experiment. The contact damping factor is a function of the coefficient of restitution of the elements in contact which can significantly change the vibration level in the bearing (Machado et al., 2012). The viscoelastic damping term in (9) is related to the coefficient of restitution, which can influence the vibration level of the bearing.

The stiffness and damping of the experimental set up was calculated by means of an impact test. Figure 6 and Figure 7

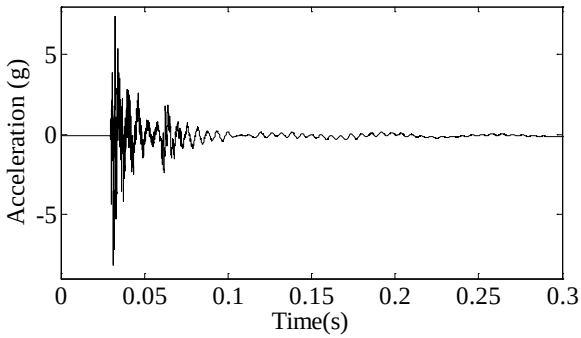

Figure 6. Time domain acceleration signal during impact test

show the time domain and frequency domain response of the acceleration signal during the impact test. Since the acceleration signal is measured in only one direction, the stiffness and damping is calculated by treating the experimental setup as a single degree of freedom system. These values are included in the bearing model to incorporate the effects of the test structure in the simulation. Calibration of the bearing contact stiffness and bearing contact damping was carried out while simulating different rotational speeds of the bearing using the model.

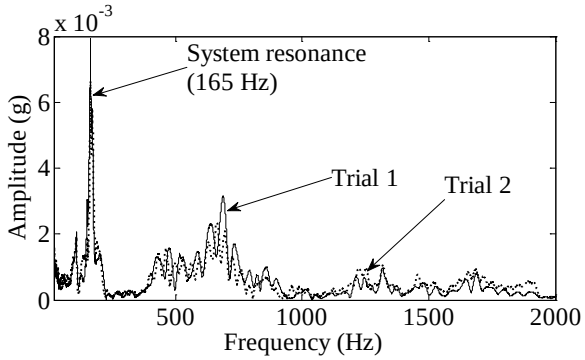

Figure 7. Frequency domain of acceleration signal during impact test.

Model calibration carried out on bearing contact damping indicated that it did not cause any significant changes in the bearing acceleration level. However, bearing contact stiffness of bearings with reduced lubricant was higher than that of the 100% bearing as shown in Figure 8. Bearing stiffness values for the 50% and 25% bearings were fairly constant indicating the boundary layer lubrication regime is exerting a significant influence on the bearing contact stiffness. This contact bearing stiffness for 50% and 25% bearings was 1.5 times that of the 100% bearing on average, as shown in Figure 9. This is in agreement with the Hertzian contact stiffness increase for boundary lubrication in comparison with hydrodynamic lubrication (Stachowiak & Batchelor, 2013).

This increase in contact stiffness due to reduction of lubricant can be used to generalize the results of this study such that the fault feature can be developed for any bearing assembly. The first step in the fault feature development is to find the global maximum of the rms acceleration level for the 100% bearing within its operating speed range, which is the numerator of the fault feature developed in this study. The second step is to use the dynamic model developed in this study to determine the bearing contact stiffness for the 100% bearing. The third step is to simulate the under-lubricated bearing case by increasing the bearing contact stiffness calculated in the previous step by a factor of 1.5. From this simulation, the global maximum of rms acceleration for an under-lubricated bearing can be identified, which is the denominator of the fault feature.

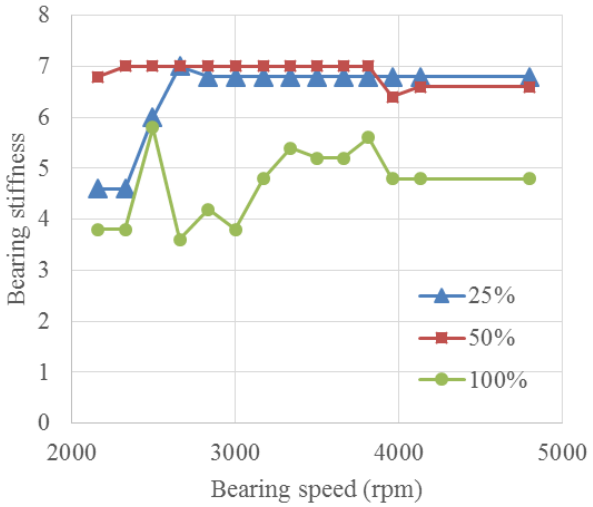

Figure 8. Bearing stiffness values for different lubricant levels and different rotational speeds

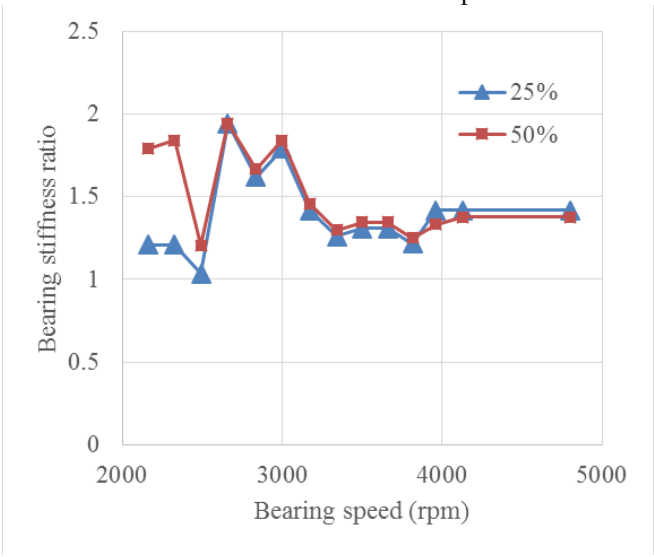

Figure 9. Ratio of bearing stiffness to the bearing stiffness of a 100% fan, at different operating speeds

Using this method, the fault feature can be developed for any bearing design, without the need to make measurements on under-lubricated bearings.

6. CONCLUSION

A fault characteristic feature to distinguish an under-lubricated bearing from a bearing with the normal amount of lubrication has been developed in this study. This feature has been developed based on the observation that the operating speed at which the maximum vibration level of the bearing is observed shifts to a different operating speed with a variation in the lubricant quantity in the bearing. This feature can be measured quickly and non-destructively, making it suitable for applications in lot acceptance or screening.

A dynamic model of a bearing was newly developed for this investigation, since existing models in the literature do not address the problem of under-lubrication in bearings. This model is used to identify the effect of the bearing contact stiffness and contact damping on the acceleration signal at various lubricant levels. Sensitivity analysis of bearing contact damping indicated that no significant changes in the bearing acceleration level are observed. The reason for this behavior could be due to the low external load acting on the bearing. Bearing contact stiffness was found to change with the reduction in the lubricant level of the bearing. The shift in vibration level with a reduction in the lubricant level in the bearing is due to the fact that the contact forces in the bearing change, resulting in a shift in the frequency domain characteristics of the dynamic system. This explained the patterns observed in the vibration level as a function of operating speed due to reduction in lubricant level in the bearing. For the 25% and 50% bearings this contact stiffness was found to be 1.5 times that of the 100% bearing. Future work anticipated on this topic will involve the validation of this classification procedure with different bearing designs and at various lubrication levels.

ACKNOWLEDGEMENT

The authors would like to thank the more than 100 companies and organizations that support research activities at CALCE at the University of Maryland annually.

REFERENCES

Boškoski, P., Petrovčič, J., Musizza, B., & Juričić, Đ. (2010). Detection of lubrication starved bearings in electrical motors by means of vibration analysis. *Tribology International*, *43*(9), 1683–1692. doi:10.1016/j.triboint.2010.03.018

Eschmann, P., Hasbargen, L., Weigand, K., & Brändlein, J. (1985). *Ball and roller bearings: Theory, design, and application*. Munich, Germany: R. Oldenbourg.

Kim, S., Vallarino, C., & Claassen, A. (1996). Review of fan life evaluation procedures. *International Journal of Reliability, Quality and Safety Engineering (IJRQSE)*, *03*(01), 75–96. doi:10.1142/S0218539396000077

Machado, M., Moreira, P., Flores, P., & Lankarani, H. M. (2012). Compliant contact force models in multibody dynamics: Evolution of the Hertz contact theory. *Mechanism and Machine Theory*, *53*, 99–121. doi:10.1016/j.mechmachtheory.2012.02.010

Morinigo-Sotelo, D., Duque-Perez, O., & Perez-Alonso, M. (2010). Assessment of the lubrication condition of a bearing using spectral analysis of the stator current. In *2010 International Symposium on Power Electronics Electrical Drives Automation and Motion (SPEEDAM)* (pp. 1160–1165). doi:10.1109/SPEEDAM.2010.5544958

Nandi, S., Toliyat, H. A., & Li, X. (2005). Condition monitoring and fault diagnosis of electrical motors-a review. *Energy Conversion, IEEE Transactions on*, *20*(4), 719 – 729. doi:10.1109/TEC.2005.847955

Ribrant, J., & Bertling, L. (2007). Survey of failures in wind power systems with focus on Swedish wind power plants during 1997-2005. In *Power Engineering Society General Meeting, 2007. IEEE* (pp. 1–8). doi:10.1109/PES.2007.386112

Sawalhi, N., & Randall, R. B. (2008). Simulating gear and bearing interactions in the presence of faults: Part I. The combined gear bearing dynamic model and the simulation of localised bearing faults. *Mechanical Systems and Signal Processing*, *22*(8), 1924–1951. doi:10.1016/j.ymssp.2007.12.001

Stachowiak, G., & Batchelor, A. W. (2014). *Engineering Tribology* (4th ed.). Oxford, U.K.: Butterworth-Heinemann.

Tandon, N., & Choudhury, A. (1999). A review of vibration and acoustic measurement methods for the detection of defects in rolling element bearings. *Tribology International*, *32*(8), 469–480. doi:10.1016/S0301-679X(99)00077-8

BIOGRAPHIES

Ranjith Kumar Sreenilayam Raveendran received his B.E. degree in mechanical engineering from the College of Engineering Guindy, Anna University, India. He is currently working toward the Ph.D. degree in mechanical engineering at the University of Maryland, College Park. He is a Graduate Research Assistant with the Center for Advanced Life Cycle Engineering, University of Maryland. His research interests include reliability, dynamics, vibration, tribology and prognostics and health management.

Michael H. Azarian received the B.S.E. degree in chemical engineering from Princeton University and the M.E. and Ph.D. degrees in materials science and engineering from Carnegie Mellon University.

He is a Research Scientist with the Center for Advanced Life Cycle Engineering (CALCE), University of Maryland, College Park. Prior to joining CALCE in 2004, he spent over 13 years in the data storage, advanced materials, and fiber optics industries. His research focuses on the analysis, detection, prediction, and prevention of failures in electronic products. He has advised many companies on reliability of electronic products, and is the author or co-author of numerous publications on solder joint degradation, electrochemical migration, capacitor reliability, electronic packaging, and tribology. He is the holder of five U.S. patents for inventions in data storage and contamination control.

Dr. Azarian is co-chair of the Miscellaneous Techniques subcommittee of the SAE G-19A standards committee on detection of counterfeit parts. He was previously the vice-chairman of the working group for IEEE Standard 1332-2012, "Reliability Program for the Development and Production of Electronic Products," and the Technical Editor of IEEE Standard 1624 on organizational reliability capability, for assessing suppliers of electronic products. He also co-chaired iNEMI's Technology Working Group on Sensor Technology Roadmapping. He is on the Editorial Advisory Board of Soldering & Surface Mount Technology.

Michael Pecht received the M.S. degree in electrical engineering and the M.S. and Ph.D. degrees in engineering mechanics from the University of Wisconsin, Madison.

He is the Founder of the Center for Advanced Life Cycle Engineering, University of Maryland, College Park, where he is also a George Dieter Chair Professor in mechanical engineering and a Professor in applied mathematics. He has been leading a research team in the area of prognostics for the past ten years and has formed a prognostics and health management consortium at the University of Maryland. He has consulted for over 100 major international electronics companies, providing expertise in strategic planning, design, test, prognostics, IP, and risk assessment of electronic products and systems. He has written more than 20 books on electronic-product development and use and supply chain management and over 400 technical articles.

Dr. Pecht is a Professional Engineer and a fellow of ASME and IMAPS. He is the editor-in-chief of IEEE Access, and served as chief editor of the IEEE Transactions on Reliability for nine years, chief editor for Microelectronics Reliability for sixteen years, an associate editor for the IEEE Transactions on Components and Packaging Technology, and on the advisory board of IEEE Spectrum. He was the recipient of the highest reliability honor, the IEEE Reliability Society’s Lifetime Achievement Award in 2008. He was also the recipient of the European Micro and Nano-Reliability Award for outstanding contributions to reliability research, the 3M Research Award for electronics packaging, and the IMAPS William D. Ashman Memorial Achievement Award for his contributions in electronics reliability analysis.